Involvement of actin polymerization in podosome dynamics

Chen Luxenburg[1,2,*], Sabina Winograd-Katz[1], Lia Addadi[2] and Benjamin Geiger[1,‡]

[1]Department of Molecular Cell Biology and [2]Department of Structural Biology, Weizmann Institute of Science, Rehovot, 76100, Israel

*Present address: Laboratory of Mammalian Cell Biology and Development, Rockefeller University, New York, NY 10065, USA

‡Author for correspondence (benny.geiger@weizmann.ac.il)

Accepted 17 November 2011
Journal of Cell Science 125, 1666–1672

doi: 10.1242/jcs.075903

Summary

Podosomes, which are formed by different monocyte derivatives, are small adhesion structures whose coordinated dynamics and cytoskeletal reorganization drive their motile and invasive features. Using live-cell microscopy, we explored the temporal molecular steps of the de novo assembly and disassembly of podosomes in cultured osteoclasts. We demonstrate here that the earliest visible step in podosome assembly is the local accumulation of the plaque protein paxillin, along with cortactin, which stabilizes actin networks, followed by robust polymerization of actin filaments and their association with α-actinin. Only then is a local increase in integrin β3 levels apparent in the podosome ring domain. Thus, local actin polymerization in cortactin- and paxillin-rich locations nucleates podosome assembly before the local accumulation of β3 integrin. We further show that actin polymerization is also important for the recruitment and maintenance of plaque proteins in the mature podosome ring domain. Our model implies that core bundle dynamics play a central role in regulating podosome stability.

Key words: Actin dynamics, Actin polymerization, Integrin adhesion, Osteoclast, Podosome, Sealing zone

Introduction

Podosomes are dynamic, actin-associated adhesion structures that are involved in the migration and matrix invasiveness of monocyte derivatives such as macrophages, dendritic cells and osteoclasts (Carman et al., 2007; Gimona and Buccione, 2006; Linder and Aepfelbacher, 2003; Tarone et al., 1985). Podosomes consist of two major structural domains: a central 'core' consisting of a tightly packed actin bundle, running perpendicular to the plasma membrane and a membrane-bound 'ring' domain, enriched with integrins and various signaling and adaptor proteins, commonly associated with cell-matrix focal adhesions (referred to here as 'plaque proteins'). The actin core is connected to the ring domain by an array of radial actin fibers, which anchor the core bundle to the plaque (Luxenburg et al., 2007). The core bundle of podosomes is enriched with several actin-associated proteins such as the actin-related protein complex 2/3 (Arp 2/3), cortactin, Wiskott–Aldrich Syndrome protein (WASp), WASP-interacting protein (WIP), dynamin and gelsolin (Linder and Aepfelbacher, 2003), which together regulate actin polymerization in the podosome core (Destaing et al., 2003). Mutation or down-regulation of these proteins is detrimental to podosome organization and function (Linder and Aepfelbacher, 2003). The mechanism underlying the effect of actin polymerization on podosome assembly is, however, by and large unclear.

In this study, we combine quantitative live-cell microscopy and high-resolution scanning electron microscopy to explore the de novo assembly and reorganization of podosomes in cultured osteoclasts. We show that this process is initiated by the local clustering of plaque proteins such as paxillin and the actin-polymerization-promoting protein cortactin, followed by growth of the actin core and an increase in β3 integrin levels in the ring domain. Attenuation of actin polymerization by cytochalasin D leads to the dissociation of plaque proteins, suggesting that actin polymerization is essential for the recruitment and maintenance of plaque components in the ring domain. Accordingly, we present a hypothetical mechanism whereby the rate of actin polymerization regulates the stability of the plaque components in the podosome ring domain.

Results

Assembly and disassembly of individual podosomes

To assess the differential rates at which podosomal components enter or exit podosomes during assembly or disassembly, RAW 264.7 monocytic cells were co-transfected with Cherry–actin and additional podosomal proteins (β3 integrin, paxillin, α-actinin or cortactin) tagged with GFP. The cells were induced to differentiate into osteoclasts, and the assembly, reorganization or disassembly of individual podosomes (Luxenburg et al., 2006b; Luxenburg et al., 2007) was monitored by live-cell microscopy (Fig. 1).

The adhesion receptor integrin αvβ3 plays a key role in osteoclast activity and in podosome-mediated signaling (McHugh et al., 2000). Simultaneous monitoring of β3 integrin and actin indicated that GFP–β3-integrin can be detected throughout the ventral membrane and is enriched in the podosome ring domain, which surrounds the actin-rich core (Fig. 1A,C; supplementary material Movie 1). However, during early stages of the de novo assembly of individual podosomes, only background GFP–β3-integrin levels could be detected before actin started to accumulate (Fig. 1A, 40 seconds). Integrins become distinctly associated with the newly forming podosome only later, usually

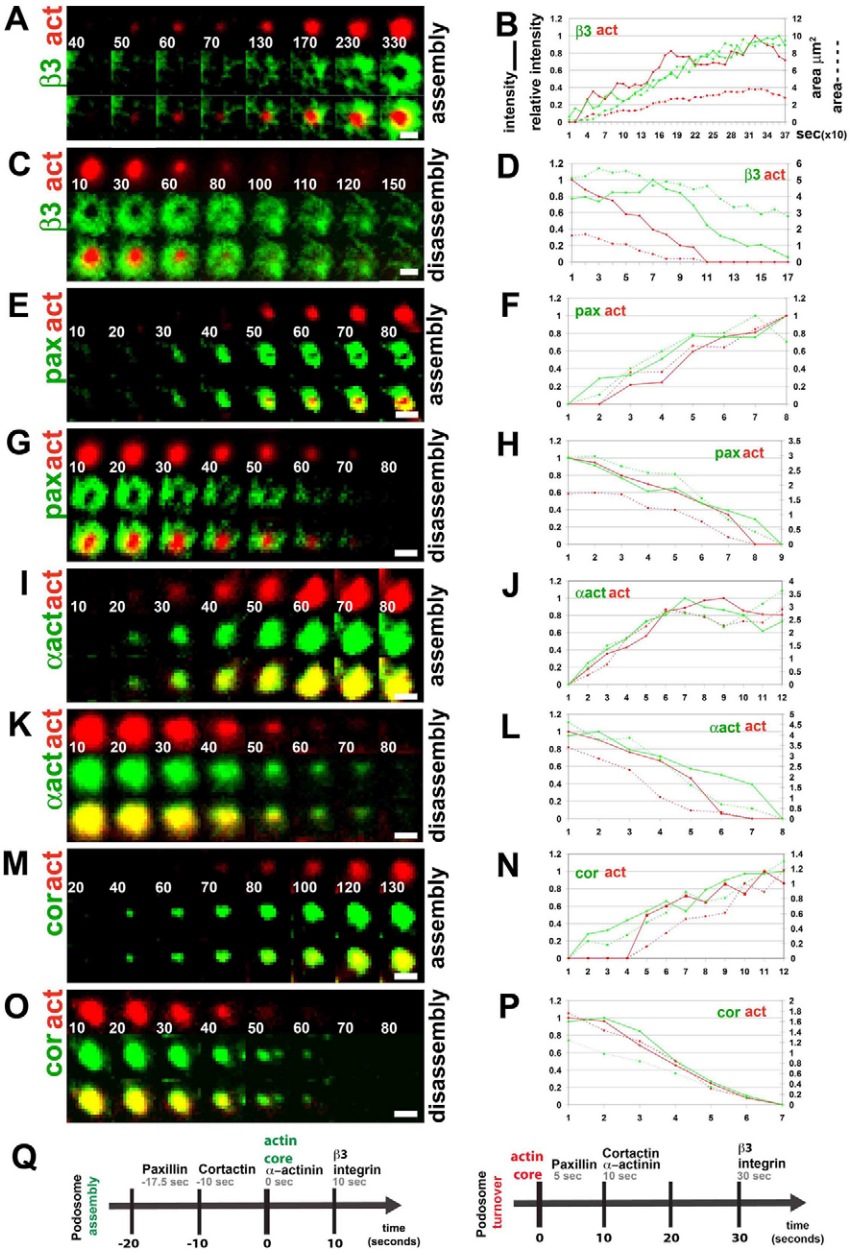

Fig. 1. Dynamic assembly and turnover of podosomes. The dynamics of osteoclasts expressing Cherry–actin and one of the following GFP-tagged proteins: β_3 integrin (**A**–**D**), paxillin (**E**–**H**), α-actinin (**I**–**L**) or cortactin (**M**–**P**), were recorded at 5- or 10-second intervals by time-lapse fluorescence microscopy. Numbers in A,C,E,G,I,K,M,O represent time in seconds. Graphs B,D,F,H,J,L,N,P present the relative intensity and the projected area of the podosomes shown in A,C,E,G,I,K,M,O, respectively. (**Q**) Assembly and turnover timelines. Time point '0' reflects the assembly or turnover of the actin core. Scale bars: 1 μm.

in the form of streaks extending radially from existing actin-rich structures (Fig. 1A, 70–130 seconds). The median time interval between the assembly of a distinct actin core and the local increase in GFP–β3-integrin levels was 10 seconds (with a range of up to 50 seconds; $n=20$). Quantitative analyses (Fig. 1B) showed that during 'maturation' of the podosome (70–330 seconds), the fluctuations in actin intensity were relatively large, which probably reflects variations in the length of the actin core bundle. By contrast, the slow, stable increase in the mean intensity and area of GFP–β3-integrin reflects the formation of a distinct, integrin-rich ring domain.

During the disassembly of individual podosomes, loss of GFP–β3-integrin from the ring domain lagged behind the disassembly of the podosome core (Fig. 1C,D; supplementary material Movie 1), with a median lag time of 20 seconds (range, up to 80 seconds; $n=20$). Upon apparent actin-core disassembly, GFP–β3-integrin first extends into the central part of the ring domain, and then slowly fades away (Fig. 1C; 80–150 seconds). Quantitative analysis of the disassembly process showed that the rapid decline in mean intensity of GFP–β3-integrin is followed by an apparent, slow decrease in the ring domain area (Fig. 1D).

Paxillin, a key adaptor protein capable of interacting with multiple constituents of the integrin adhesome (Zaidel-Bar et al., 2007; Zaidel-Bar and Geiger, 2010), localizes to the ring domain surrounding the Cherry–actin core (Fig. 1E,G; supplementary material Movie 2, Fig. S1). During the de novo assembly of podosomes, an elongated paxillin-containing structure (~0.5–1 μm) is consistently seen, before the formation of a distinct actin core (Fig. 1E; 20–40 seconds). The median lag period between the appearance of the first paxillin structure and the actin core is

17.5 seconds (range, up to 50 seconds; $n=30$). However, the development of a mature paxillin ring occurs only after the assembly of the actin core (Fig. 1E, 50–80 seconds; supplementary material Fig. S1). During the disassembly of individual podosomes, the disappearance of GFP–paxillin lagged slightly behind the decline of Cherry–actin (Fig. 1G,H; median lag time, 5 seconds; range, up to 40 seconds; $n=30$).

α-Actinin is an actin-bundling protein that can also interact directly with integrins (Matsudaira, 1994). Examination of cells expressing GFP–α-actinin and Cherry–actin revealed a close similarity in the distribution of the two proteins (Fig. 1I–L). During the de novo assembly of podosomes, a dot-like GFP–α-actinin structure appeared, essentially simultaneously with the formation of the Cherry–actin core (Fig. 1I; 20 seconds), suggesting that in newly formed podosomes, α-actinin readily crosslinks polymerizing actin into a bundle. The median interval between the assembly of the two proteins was <1 second (range, up to 10 seconds; $n=40$). During the disassembly of podosomes, a reduction in GFP–α-actinin levels lagged behind the decline of Cherry–actin (Fig. 1K; 60–80 seconds), with a median delay of about 10 seconds (range, up to 30 seconds; $n=33$). Quantitative analyses of GFP–α-actinin and Cherry–actin showed that both the mean intensity and area of the two proteins are closely inter-correlated during podosome assembly and maintenance (Fig. 1J,L).

Cortactin is an actin nucleation-promoting and F-actin stabilizer protein in podosomes that is essential for podosome assembly (Tehrani et al., 2006), and it colocalizes with Cherry–actin at the podosome core (Fig. 1M,O). During podosome assembly, a GFP–cortactin dot is apparent before the increase in Cherry–actin assembly (Fig. 1M,N; 20–60 seconds). The median time interval between the appearance of GFP–cortactin and the onset of actin polymerization was 10 seconds (range, up to 40 seconds; $n=33$), in line with previous findings (Kaverina et al., 2003). During podosome disassembly (Fig. 1O,P), the decline in GFP–cortactin levels lagged slightly behind that of Cherry–actin, with a mean lag time of 10 seconds (range, up to 40 seconds; $n=25$). Taken together, these results suggest that an individual podosome formation involves an early local accumulation of paxillin, nucleation/stabilization of actin by cortactin and its bundling by α-actinin, followed by a major increase β3 integrin levels.

The role of actin polymerization and myosin II motor activity in podosome dynamics and molecular organization

The data described above suggest that actin dynamics play a role in podosome formation. Is local actin polymerization and myosin-II-driven contractility also important for the molecular composition and stability of mature podosomes? Previous studies established that podosomes are highly dynamic structures, and that their actin cores undergo continuous polymerization and severing processes (Linder and Aepfelbacher, 2003). Fluorescence recovery after photobleaching (FRAP) analysis revealed that actin dynamics are regulated by a variety of podosome-associated proteins, including $pp60^{src}$ (Destaing et al., 2008), dynamin (Ochoa et al., 2000) and pyk2 (Gil-Henn et al., 2007); yet the direct impact of actin dynamics on the overall structure and stability of podosomes remains unclear.

To address this issue, we experimentally modulated actin dynamics and myosin II activity in cultured osteoclasts, and monitored the effects of this perturbation on the molecular and structural integrity of the podosome. To measure the rate of actin polymerization in podosomes, we performed FRAP measurements on osteoclasts expressing GFP–actin. Individual or clustered podosome cores were photobleached, and the rate of actin recovery was calculated. The average photobleaching recovery time in control cells was 27±6 seconds (Fig. 2A,B). To modulate the actin polymerization rate, we used cytochalasin D (CD), which caps the barbed ends of actin filaments and slows the rate of actin polymerization (Galbraith et al., 2007). Indeed, treatment of osteoclasts with 50 nM or 150 nM CD resulted in an increase in FRAP time of 42.0±9.5 and 56.0±10 seconds, respectively

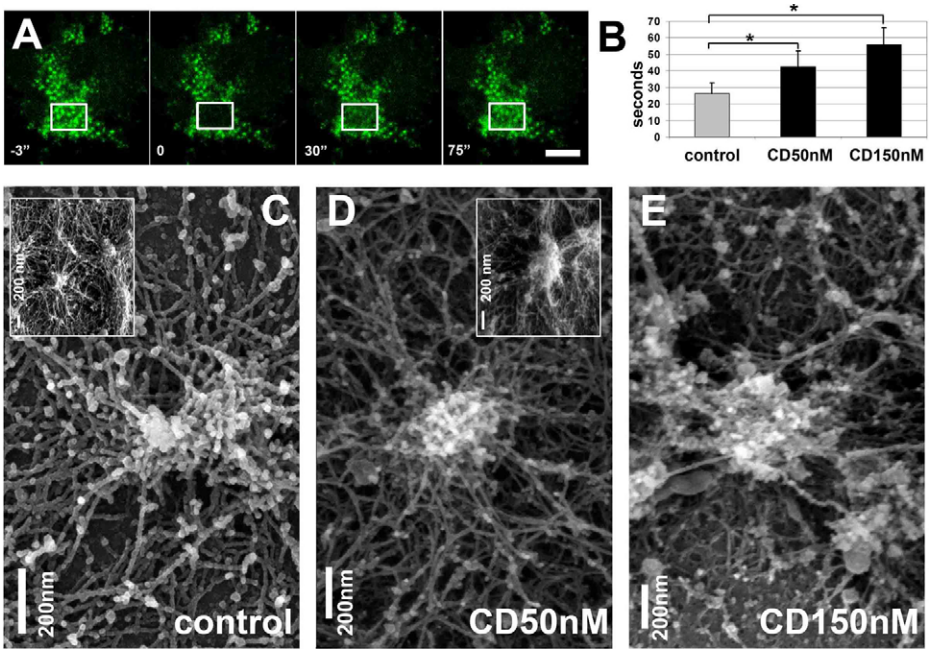

Fig. 2. Actin polymerization affects the structural organization of podosomes. (**A**,**B**) Osteoclasts expressing GFP–actin were analyzed by FRAP. (A) White boxes indicate the area that was photobleached. Scale bar: 10 μm. (B) The characteristic FRAP time measured in control and cytochalasin D (CD)-treated cells (*$P<0.005$). (**C**–**E**) Cells were treated with 0.01% DMSO (C), 50 nM CD (D) or 150 nM CD (E) and podosomes were visualized by HR-SEM. Insets in C and D show HR-SEM micrograph taken at 40° tilt. Note normal (C,D) vs abnormal (E) podosomal architecture.

(Fig. 2B; *$P<0.005$). To determine the effect of actin polymerization on the structural organization of podosomes, osteoclasts were treated with 50 nM or 150 nM CD for 15 minutes (control cells were treated with 0.01% DMSO), and processed for observation by high-resolution scanning electron microscopy (HR-SEM) (Luxenburg et al., 2007). A tilted (40°) view of podosomes from control cells confirmed their typical three-dimensional architecture (Fig. 2C, insert). Cells treated with 50 nM CD maintained apparently normal organization (Fig. 2D), despite the slower rate of actin turnover in their cores. By contrast, actin in podosomes of cells treated with 150 nM CD was abnormal: the central bundle was less ordered and the number of radial actin cables was markedly reduced (Fig. 2E). Modulation of actin dynamics by jasplakinolide (1 μM for up to 10 minutes), a potent actin-stabilizing microlide (Galbraith et al., 2007), which blocks actin dynamics in podosomes, caused a dramatic collapse of podosomes onto the osteoclast ventral membrane, resulting in a nearly two-dimensional layer of long and intertwined fibers (supplementary material Fig. S2). By contrast, treatment with 50 μM blebbistatin for 15 minutes did not affect the overall structural organization of individual podosomes (supplementary material Fig. S3).

To further assess the role of actin polymerization and myosin II motor activity in individual or clustered podosome dynamics, we measured the effect of CD and blebbistatin treatment on the average lifespan of actin in such podosomes, using live-cell microscopy. As shown in Fig. 3A,B, treatment with 50 nM CD doubled the average podosomal lifespan from 172±78 seconds in control cells to 358±185 seconds ($P<0.005$), whereas blebbistatin treatment had no effect (181±89 seconds). These results indicate that mild attenuation of actin polymerization, rather than actomyosin contractility, dramatically suppresses turnover of individual or clustered podosomes, without altering their three-dimensional structure.

The apparent effect of attenuation of actin polymerization on podosome dynamics raised the possibility that actin dynamics might affect the structure and stability of the adhesive ring domain that surrounds the podosome actin core. Previous studies indicated that the podosomal actin system is tightly associated with the plasma membrane at two distinct sites: a thin membrane invagination that penetrates into the core bundle (Ochoa et al., 2000) and the ring domain, associated with the radial actin fibers (Luxenburg et al., 2007). To probe the possible role of actin flux in regulating the ring domain of podosomes, we tested the effect of 50 nM CD on the levels of a variety of podosome components. In the first series of experiments, cells expressing Cherry–actin and either GFP–paxillin or GFP–β3-integrin were visualized by time-lapse microscopy. Data were collected for 20 minutes with no treatment, followed by the addition of 50 nM CD, after which the cells were inspected for an additional 20 minutes. An apparent decrease in the local intensity of GFP–paxillin associated with the podosome ring domain was observed within 2–3 minutes after addition of the drug (Fig. 3C; supplementary material Movie 3). By contrast, no apparent change was noted in the distribution or intensity of GFP–β3-integrin within the timeframe of these experiments (data not shown).

To quantify the effect of actin modulation on additional podosome components, osteoclasts were treated with 50 nM CD (or 0.01% DMSO, as a control) for 15 minutes, fixed and immunostained for F-actin and either vinculin, paxillin, α-actinin or Arp3. Using quantitative fluorescence microscopy, the ratio between the total actin intensity at the podosome core and the intensity values measured for each of the associated proteins was calculated. Treatment with 50 nM CD for 15 minutes did not alter the average podosome-associated total actin intensity (Fig. 3D). However, vinculin and paxillin levels in the ring domain decreased by 39% and 30%, respectively. By contrast, treatment with CD increased Arp3 levels by 28%, although

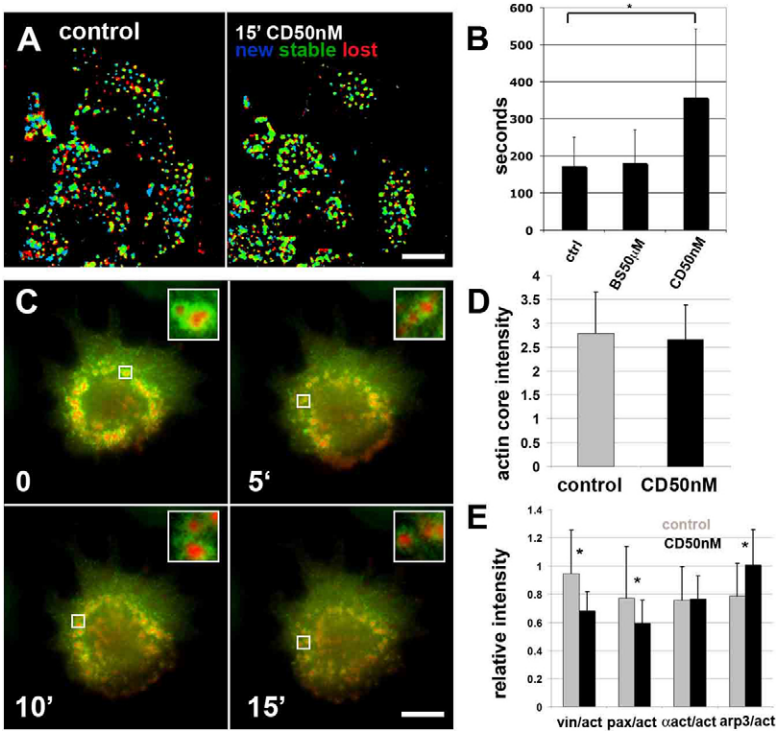

Fig. 3. Actin polymerization regulates podosome dynamics and molecular composition. (**A**) Temporal ratio imaging of a cell expressing GFP–actin before (control) and after 15 minutes of treatment with 50 nM CD. Notice the increase in stable structures. Scale bar: 10 μm. (**B**) Average podosome lifespan ± s.d. (*$P<0.005$). (**C**) Cells co-expressing Cherry–actin and GFP–paxillin were treated with 50 nM CD. Notice the decrease in paxillin association with podosomes: insert shows 3× digital magnification. Scale bar: 10 μm. (**D**) Total actin intensity of podosomes in control cells and in cells treated with 50 nM CD. (**E**) The ratio between the net intensities of a podosome-associated protein and actin, in control cells and in cells treated with 50 nM CD (*$P<0.005$).

α-actinin levels were not affected (Fig. 3E). At present, the precise molecular mechanism underlying the intriguing loss of podosomal plaque proteins (and hence deterioration of podosomes) following attenuation of actin polymerization is poorly understood; yet it is tempting to propose that mechanical forces, applied by the treadmilling actin core filaments to the 'lateral' F-actin, which is anchored to the adhesion plaque of the podosomal ring domain (see below), might regulate the stability of the adhesion ring. Such a mechanism is reminiscent of the effect of relaxation of actomyosin contractility on the integrity of another type of integrin adhesion, namely, focal adhesions (Geiger et al., 2001). The mechanosensitivity of focal adhesions was shown to respond to both external or cytoskeletal tension and to be regulated by the small GTPase RhoA (Geiger et al., 2009; Riveline et al., 2001). To test whether the loss of paxillin and vinculin from the podosome plaque was also sensitive to changes in actomyosin-induced contractility, we treated osteoclasts with 50 μM blebbistatin for 60 minutes and monitored both actin and vinculin levels in individual or clustered podosomes. In contrast to focal adhesions, this treatment had only a subtle effect on vinculin recruitment into these podosomes (supplementary material Fig. S3).

Discussion

In this study, we have used live-cell microscopy to study molecular processes associated with the assembly and disassembly of podosomes in cultured osteoclasts. The results presented herein point to two major novel features that deserve additional discussion here, namely the order of recruitment of specific associated proteins during podosome formation and dissociation, and the role of actin polymerization in maintaining the structural integrity of podosomes. Taken together, the observations reported here indicate that the de novo assembly of individual podosomes occurs in three major temporal steps: (1) local accumulation of paxillin and cortactin; (2) nucleation and polymerization of the actin core fibers, consolidated by their association with α-actinin; and (3) massive recruitment of αvβ3 integrins into a ring surrounding the actin core. The late timing of the β3 integrin enrichment is surprising, in view of previous reports suggesting that this integrin is crucial for the formation of other integrin adhesions, such as cell–extracellular-matrix (ECM) focal adhesions (Zaidel-Bar et al., 2003). Several possible explanations could account for this phenomenon: it is possible that low, 'background levels' of β3 integrin are sufficient to support local adhesion to the matrix, whereas subsequent growth and extension of the integrin domain is necessary for membrane anchoring of the radial actin filaments, or formation of higher-order adhesions (e.g. sealing zones). Such activity might be analogous to the transition from nascent adhesions to focal complexes to focal adhesions in fibroblasts, a process believed to be initially driven by actin flow, and later regulated by mechanical forces generated by the cellular contractile machinery (Wolfenson et al., 2009). Alternatively, the initial adhesion to the matrix might occur by means of adhesion through receptors other than β3 integrin, such as α2β1 or αv β1 (Ross and Teitelbaum, 2005), which could, in principle, mediate the initial stages of podosome assembly.

Examination of integrin expression by both microarray analysis (M. Mann, E. Hornstein and B.G. unpublished data) and immunofluorescence indicated that α5 integrin is expressed in differentiating RAW cells (supplementary material Fig. S4). However, pre-treatment of the cells with integrin α5 inhibitory antibodies had no apparent effect on the formation of podosomes (supplementary material Fig. S5) and their subsequent assembly into sealing zones. The same antibodies strongly suppressed the formation of focal adhesions by cultured fibroblasts.

Finally, it is possible that the early stages of podosome assembly have an inside-out element, involving F-actin, actin-associated proteins and adhesion plaque components (e.g. paxillin). That said, it is important to note that podosome formation depends on the presence of physiological ECM components (e.g. vitronectin) on the surface, because plating osteoclasts on poly-lysine-coated substrates failed to induce podosome assembly (supplementary material Fig. S6). Furthermore, addition of a soluble form of the cyclic adhesive peptide c(RGD) (Arnold et al., 2004) inhibits podosome formation on adhesive substrates. These additional results confirm that the essential steps of podosome assembly are indeed integrin mediated. It is noteworthy that assembly of invadopodia or podosomes by Rous sarcoma virus (RSV)-transformed baby hamster kidney (BHK) cells is initiated by the formation of an actin-rich core, before the recruitment of integrins and plaque proteins (Badowski et al., 2008), in line with the late enrichment of integrins into podosomes. Thus, an apparent inside-out process might exist in other podosomal systems, although variations in the order of recruitment of specific molecules during podosome assembly could occur as a result of a different podosome-induction mechanism, or due to genuine differences between osteoclasts podosomes and Src-induced podosomes and invadopodia.

The other observation reported here is the high sensitivity of the podosomal plaque to low CD concentrations, which are sufficient to slow down actin polymerization, yet do not destroy the filaments. Interestingly, actomyosin motor inhibition, which is detrimental to focal adhesions, had essentially no effect on the formation or stability of individual podosomes. These observations suggest a novel mechanism for the mechanical regulation of integrin-mediated adhesions. Taking into account the fact that actin polymerization in the core bundle occurs by addition of actin monomers at the bundle–membrane interface (Linder and Aepfelbacher, 2003), one could suggest a possible process whereby 'centripetal treadmilling' of the core actin bundle generates opposing mechanical forces at the interfaces between core bundles and the membrane and radial fibers and the membrane. Thus, we envisage that the elongating core might push against the ventral membrane, whereas the stretched radial fibers might pull on the vinculin- and paxillin-rich plaque of the ring domain (Fig. 4). Consequently, a complex micro-system of mechanical forces would ensue, which could directly affect podosome formation and turnover. Such a mechanism might be similar to the one affecting focal adhesions, in the sense that both are regulated by mechanical forces, despite the fact that the forces generated in the two systems are produced by distinct molecular machineries (actin polymerization, in the case of podosomes and actomyosin contractility in the stress fiber and focal adhesion system).

It is noteworthy that there was essentially no apparent effect of actomyosin inhibition on the structure of individual or clustered podosomes in cultured RAW osteoclasts. However, when Rho activity was reduced by exoenzyme C3, sealing zones of matrix degrading osteoclasts were replaced by a loose belt of podosomes (Saltel et al., 2004), in which the inter-podosome spacing was

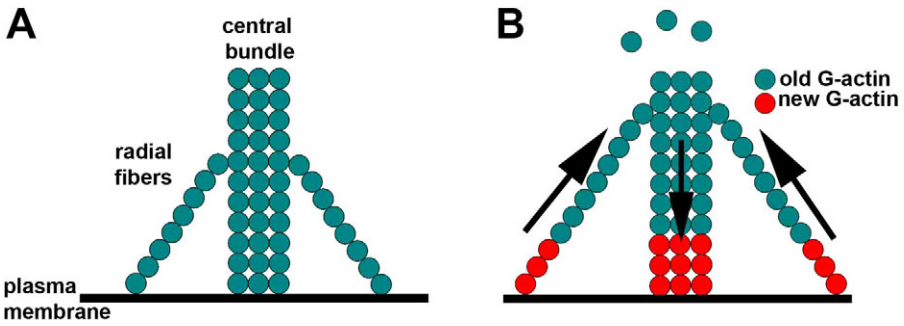

Fig. 4. A model for the involvement of actin-polymerization-derived mechanical forces in plaque recruitment. (**A**) Podosomes contain a central actin bundle, which is associated with radial actin fibers that interact, at their other ends, with the membrane-bound podosome plaque. (**B**) These two actin-based domains undergo polymerization at a similar rate: actin monomers are inserted at the membrane-bound end, and dissociate from the other end of the fibers. Here, we raise the possibility that the radial fibers, attached at one end to the treadmilling core bundle, and at the other end to the membrane-associated plaque, are under tension driven by actin polymerization, and apply this tension to the plaque. According to this model, forces originating from actin polymerization and acting on the actin-membrane interfaces of the core bundle and radial fibers, act in opposite directions for reasons of geometry: at equal extension rates, the central bundle pushes against the membrane, whereas the radial fibers pull on the plaque proteins of the ring domain.

larger than that found in mature sealing zone (Luxenburg et al., 2007). These observations suggest a role for myosin II activity in sealing zone 'condensation' or 'compaction'. Indeed, we have previously shown that podosomes change their dynamic properties, molecular composition and structural organization as they mature from individual adhesion structures into belts or sealing zones (Luxenburg et al., 2006a; Luxenburg et al., 2006b; Luxenburg et al., 2007). Additional studies are needed to understand the mechanisms whereby myosin II motor activity affects the assembly of podosomal super structures.

Moreover, there is evidence that myosin II has a key role in podosome formation in other experimental systems. In dendritic cells, for example, prostaglandin E2 treatment promotes actomyosin-derived contractility, which eventually replaces podosomes by focal adhesion (van Helden et al., 2008). By contrast, in cultured macrophages, myosin IIA motor activity promotes podosome assembly (Kopp et al., 2006), and regulates their stiffness and height (Labernadie et al., 2010). The basis for this apparent discrepency is not clear and might be attributed to cell-type-specific variations. Further explorations into how actin polymerization and actomyosin contractility differentially affect podosome assembly and the development of adhesion super-structures might shed light on the basis of these differences.

Materials and Methods

cDNA, antibodies and reagents

GFP–actin (Ballestrem et al., 1998), GFP–paxillin (Zamir et al., 2000), GFP–α3-integrin (Ballestrem et al., 2001), GFP–cortactin (Kaksonen et al., 2000), Cherry–actin and Cherry–paxillin were generous gifts from Vic Small (Institute of Molecular Biology, Austrian Academy of Sciences, Salzburg, Austria). GFP–α-actinin was a generous gift from Carol A. Otey (University of North Carolina, Chapel Hill, NC).

Primary antibodies used included: monoclonal anti-vinculin (clone hVin-1, Sigma, St Louis, MO), monoclonal anti-a-actinin (clone 75.2, Sigma) monoclonal anti-paxillin and monoclonal anti-Arp3 (BD Transduction Laboratories, San Jose, CA), anti-integrin-α5 antibody [5H10-27 (MFR5)] and anti-HA tag [12CA5] (Abcam, Cambridge, MA). The secondary antibody used was goat anti-mouse IgG conjugated to Alexa Fluor 488 (Invitrogen, Carlsbad, CA), Actin was labeled with phalloidin conjugated to TRITC (Sigma); cytochalasin D was from Sigma and jasplakinolide, from Calbiochem (San Diego, CA).

Cell culture, transfection, fixation and staining

RAW 264.7 cells were obtained from the American Type Culture Collection (Manassas, VA). RAW 264.7 cells stably expressing GFP–actin were previously described (Luxenburg et al., 2006b). To induce osteoclast differentiation, 100 cells/mm^2 were grown at 37℃ in a 5% CO_2 humidified atmosphere for 3 days in alpha MEM with Earle's salts, L-glutamine and $NaHCO_3$ (Sigma) supplemented with 10% fetal bovine serum (FBS) (Gibco, Grand Island, NY) and antibiotics (Biological Industries, Beit Haemek, Israel), 20 ng/ml recombinant soluble receptor activator of NFκB ligand (RANK-L) and 20 ng/ml of macrophage colony-stimulating factor (mCSF), both from R&D (Minneapolis, MN).

After 48 hours of differentiation, transfection was conducted with Lipofectamine 2000 (Invitrogen). Cells were allowed to differentiate for an additional 30 hours, and then assayed. Immunolabeling was performed, as previously described (Luxenburg et al., 2006a). Briefly, cells were fixed for 2 minutes in warm 3% paraformaldehyde (PFA) (Merck, Darmstadt, Germany) + 0.5% Triton X-100 (Sigma), and then in PFA alone for an additional 40 minutes. After fixation, cells were washed three times with PBS, pH 7.4, and incubated with primary antibody for 40 minutes, washed again three times in PBS, and incubated for an additional 40 minutes with secondary antibodies.

Image acquisition, live-cell imaging and electron microscopy

Movies and fixed cell data were acquired with a DeltaVision-RT system (Applied Precision, Issaquah, WA), consisting of an inverted microscope IX71 equipped with 100×/1.4 NA objectives (Olympus, Tokyo, Japan) and with a temperature-controlled box using Resolve3D software (Applied Precision). For live-cell imaging, RAW cells were induced to differentiate in 35 mm glass-bottomed dishes; medium was then changed to DMEM containing 25 mM HEPES without Phenol Red, and riboflavin (Biological Industries), and supplemented with 10 ng/ml mCSF and 10 ng/ml RANKL. Fluorescence recovery after photobleaching (FRAP) data were acquired with a Zeiss LSM510 confocal microscope, using a 63×/1.4 NA objective (Zeiss).

Ventral membrane preparation (VMP) for electron microscopy was undertaken as previously described (Luxenburg et al., 2007). Briefly, the method involves the mechanical removal of the cell body while leaving the ventral membrane intact, followed by fixation with warm 2% glutaraldehyde (GA) (EMS, Hatfield, PA) and post-fixation with 1% OsO_4 (EMS) and 1% tannic acid (Merck). VMPs were then dehydrated in an ethanol series, followed by critical-point drying using CPD30 (Bal-Tec, Blazers, Lichtenstein), coated with 2 nm Cr using K575X (EMITEC). Samples were visualized with a high-resolution SEM Ultra 55 (Zeiss).

Image analysis and statistics

To trace podosome assembly and disassembly, two-color movies were collected at intervals of 5 or 10 seconds. The delay between the red and the green channels is less than 1 second in the Delta Vision-RT system. Prism software for Linux operating systems (msg.ucsf.edu/IVE/Download/) was used to high-pass filter images (Zamir et al., 1999) and individual podosomes were traced within each frame. FRAP analyses were carried out with LSM 510 software (Zeiss).

The polygon tool in the WoRX software (Applied Precision) was used to calculate the mean fluorescence intensity and area. To calculate net intensity of selected staining, RAW cells were induced to differentiate into osteoclasts, treated with 0.01% DMSO, 50 nM CD or 50 μM blebbistatin for 15 minutes, fixed and co-stained for actin and an additional protein of interest. Treated cells were always processed in parallel with controls. Individual or cluster podosomes were marked by polygons, and the mean intensity and area were measured. Background mean intensity was calculated for every measurement, and juxtaposed onto the selected

structure, using the same size of polygon. Total actin intensity represents the ratio between F-actin mean intensity at the podosome core, and its background (outside the actin cloud). The same calculation was used to determine the net intensity of the additional proteins.

Data were collected from at least three independent preparations. For all quantified data, mean ± s.d. was presented. To determine significance between two groups, indicated in figures by an asterisk, comparisons were made using the Student's *t*-test. For all statistical tests, the 0.05 level of confidence was accepted for statistical significance.

Acknowledgements

We would like to thank Barbara Morgenstern for expert editorial assistance. B.G. holds the Erwin Neter Professorial Chair in Cell and Tumor Biology. L.A. holds the Dorothy and Patrick E. Gorman Professorial Chair of Biological Ultrastructure.

Funding

This study was supported by a grant from the Israel Science Foundation to L.A. and B.G.; the T3Net project of the EU-FP7 program; and a National Institutes of Health NIGMS grant from the Cell Migration Consortium [grant number U54GM64346]. Deposited in PMC for release after 12 months.

Supplementary material available online at
http://jcs.biologists.org/lookup/suppl/doi:10.1242/jcs.075903/-/DC1

References

Arnold, M., Cavalcanti-Adam, E. A., Glass, R., Blummel, J., Eck, W., Kantlehner, M., Kessler, H. and Spatz, J. P. (2004). Activation of integrin function by nanopatterned adhesive interfaces. *ChemPhysChem* **5**, 383-388.

Badowski, C., Pawlak, G., Grichine, A., Chabadel, A., Oddou, C., Jurdic, P., Pfaff, M., Albigès-Rizo, C. and Block, M. R. (2008). Paxillin phosphorylation controls invadopodia/podosomes spatiotemporal organization. *Mol. Biol. Cell* **19**, 633-645.

Ballestrem, C., Wehrle-Haller, B. and Imhof, B. A. (1998). Actin dynamics in living mammalian cells. *J. Cell Sci.* **111**, 1649-1658.

Ballestrem, C., Hinz, B., Imhof, B. A. and Wehrle-Haller, B. (2001). Marching at the front and dragging behind: differential alphaVbeta3-integrin turnover regulates focal adhesion behavior. *J. Cell Biol.* **155**, 1319-1332.

Carman, C. V., Sage, P. T., Sciuto, T. E., de la Fuente, M. A., Geha, R. S., Ochs, H. D., Dvorak, H. F., Dvorak, A. M. and Springer, T. A. (2007). Transcellular diapedesis is initiated by invasive podosomes. *Immunity* **26**, 784-797.

Destaing, O., Saltel, F., Geminard, J. C., Jurdic, P. and Bard, F. (2003). Podosomes display actin turnover and dynamic self-organization in osteoclasts expressing actin-green fluorescent protein. *Mol. Biol. Cell* **14**, 407-416.

Destaing, O., Sanjay, A., Itzstein, C., Horne, W. C., Toomre, D., De Camilli, P. and Baron, R. (2008). The tyrosine kinase activity of c-Src regulates actin dynamics and organization of podosomes in osteoclasts. *Mol. Biol. Cell* **19**, 394-404.

Galbraith, C. G., Yamada, K. M. and Galbraith, J. A. (2007). Polymerizing actin fibers position integrins primed to probe for adhesion sites. *Science* **315**, 992-995.

Geiger, B., Bershadsky, A., Pankov, R. and Yamada, K. M. (2001). Transmembrane crosstalk between the extracellular matrix and the cytoskeleton. *Nat. Rev. Mol. Cell Biol.* **2**, 793-805.

Geiger, B., Spatz, J. P. and Bershadsky, A. D. (2009). Environmental sensing through focal adhesions. *Nat. Rev. Mol. Cell Biol.* **10**, 21-33.

Gil-Henn, H., Destaing, O., Sims, N. A., Aoki, K., Alles, N., Neff, L., Sanjay, A., Bruzzaniti, A., De Camilli, P., Baron, R. et al. (2007). Defective microtubule-dependent podosome organization in osteoclasts leads to increased bone density in Pyk2(-/-) mice. *J. Cell Biol.* **178**, 1053-1064.

Gimona, M. and Buccione, R. (2006). Adhesions that mediate invasion. *Int. J. Biochem. Cell Biol.* **38**, 1875-1892.

Kaksonen, M., Peng, H. B. and Rauvala, H. (2000). Association of cortactin with dynamic actin in lamellipodia and on endosomal vesicles. *J. Cell Sci.* **113**, 4421-4426.

Kaverina, I., Stradal, T. E. and Gimona, M. (2003). Podosome formation in cultured A7r5 vascular smooth muscle cells requires Arp2/3-dependent de-novo actin polymerization at discrete microdomains. *J. Cell Sci.* **116**, 4915-4924.

Kopp, P., Lammers, R., Aepfelbacher, M., Woehlke, G., Rudel, T., Machuy, N., Steffen, W. and Linder, S. (2006). The kinesin KIF1C and microtubule plus ends regulate podosome dynamics in macrophages. *Mol. Biol. Cell* **17**, 2811-2823.

Labernadie, A., Thibault, C., Vieu, C., Maridonneau-Parini, I. and Charrière, G. M. (2010). Dynamics of podosome stiffness revealed by atomic force microscopy. *Proc. Natl. Acad. Sci. USA* **107**, 21016-21021.

Linder, S. and Aepfelbacher, M. (2003). Podosomes: adhesion hot-spots of invasive cells. *Trends Cell Biol.* **13**, 376-385.

Luxenburg, C., Addadi, L. and Geiger, B. (2006a). The molecular dynamics of osteoclast adhesions. *Eur. J. Cell Biol.* **85**, 203-211.

Luxenburg, C., Parsons, J. T., Addadi, L. and Geiger, B. (2006b). Involvement of the Src-cortactin pathway in podosome formation and turnover during polarization of cultured osteoclasts. *J. Cell Sci.* **119**, 4878-4888.

Luxenburg, C., Geblinger, D., Klein, E., Anderson, K., Hanein, D., Geiger, B. and Addadi, L. (2007). The architecture of the adhesive apparatus of cultured osteoclasts: from podosome formation to sealing zone assembly. *PLoS ONE* **2**, e179.

Matsudaira, P. (1994). The fimbrin and alpha-actinin footprint on actin. *J. Cell Biol.* **126**, 285-287.

McHugh, K. P., Hodivala-Dilke, K., Zheng, M. H., Namba, N., Lam, J., Novack, D., Feng, X., Ross, F. P., Hynes, R. O. and Teitelbaum, S. L. (2000). Mice lacking beta3 integrins are osteosclerotic because of dysfunctional osteoclasts. *J. Clin. Invest.* **105**, 433-440.

Ochoa, G. C., Slepnev, V. I., Neff, L., Ringstad, N., Takei, K., Daniell, L., Kim, W., Cao, H., McNiven, M., Baron, R. et al. (2000). A functional link between dynamin and the actin cytoskeleton at podosomes. *J. Cell Biol.* **150**, 377-389.

Riveline, D., Zamir, E., Balaban, N. Q., Schwarz, U. S., Ishizaki, T., Narumiya, S., Kam, Z., Geiger, B. and Bershadsky, A. D. (2001). Focal contacts as mechanosensors: externally applied local mechanical force induces growth of focal contacts by an mDia1-dependent and ROCK-independent mechanism. *J. Cell Biol.* **153**, 1175-1186.

Ross, F. P. and Teitelbaum, S. L. (2005). alphavbeta3 and macrophage colony-stimulating factor: partners in osteoclast biology. *Immunol. Rev.* **208**, 88-105.

Saltel, F., Destaing, O., Bard, F., Eichert, D. and Jurdic, P. (2004). Apatite-mediated dynamics in resorbing osteoclasts. *Mol. Biol. Cell* **15**, 5231-5241

Tarone, G., Cirillo, D., Giancotti, F. G., Comoglio, P. M. and Marchisio, P. C. (1985). Rous sarcoma virus-transformed fibroblasts adhere primarily at discrete protrusions of the ventral membrane called podosomes. *Exp. Cell Res.* **159**, 141-157.

Tehrani, S., Faccio, R., Chandrasekar, I., Ross, F. P. and Cooper, J. A. (2006). Cortactin has an essential and specific role in osteoclast actin assembly. *Mol. Biol. Cell* **17**, 2882-2895.

van Helden, S. F., Oud, M. M., Joosten, B., Peterse, N., Figdor, C. G. and van Leeuwen, F. N. (2008). PGE2-mediated podosome loss in dendritic cells is dependent on actomyosin contraction downstream of the RhoA-Rho-kinase axis. *J. Cell Sci.* **121**, 1096-1106.

Wolfenson, H., Henis, Y., Geiger, B. and Bershadsky, A. (2009). The heel and toe of the cell's foot: A multifaceted approach for understanding the structure and dynamics of focal adhesions. *Cell Motil. Cytoskeleton* **66**, 1017-1029.

Zaidel-Bar, R. and Geiger, B. (2010). The switchable integrin adhesome. *J. Cell Sci.* **123,** 1385-1388.

Zaidel-Bar, R., Ballestrem, C., Kam, Z. and Geiger, B. (2003). Early molecular events in the assembly of matrix adhesions at the leading edge of migrating cells. *J. Cell Sci.* **116**, 4605-4613.

Zaidel-Bar, R., Milo, R., Kam, Z. and Geiger, B. (2007). A paxillin tyrosine phosphorylation switch regulates the assembly and form of cell-matrix adhesions. *J. Cell Sci.* **120**, 137-148.

Zamir, E., Katz, B. Z., Aota, S., Yamada, K. M., Geiger, B. and Kam, Z. (1999). Molecular diversity of cell-matrix adhesions. *J. Cell Sci.* **112**, 1655-1669.

Zamir, E., Katz, M., Posen, Y., Erez, N., Yamada, K. M., Katz, B. Z., Lin, S., Lin, D. C., Bershadsky, A., Kam, Z. et al. (2000). Dynamics and segregation of cell-matrix adhesions in cultured fibroblasts. *Nat. Cell Biol.* **2**, 191-196.